JACS
JOURNAL OF THE AMERICAN CHEMICAL SOCIETY
Communication
pubs.acs.org/JACS

Bidenticity-Enhanced Second Harmonic Generation from Pb Chelation in $Pb_3Mg_3TeP_2O_{14}$

Hongwei Yu,[†] Weiguo Zhang,[†] Joshua Young,[‡,§] James M. Rondinelli,*[,‡] and P. Shiv Halasyamani*[,†]

[†]Department of Chemistry, University of Houston, 112 Fleming Building, Houston, Texas 77204-5003, United States

[‡]Department of Materials Science and Engineering, Northwestern University, 2220 Campus Drive, Evanston, Illinois 60208-3108, United States

[§]Department of Materials Science and Engineering, Drexel University, 3141 Chestnut Street, Philadelphia, Pennsylvania 19102, United States

Supporting Information

ABSTRACT: A new ultraviolet nonlinear optical (NLO) material, $Pb_3Mg_3TeP_2O_{14}$ (PMTP), has been synthesized and characterized. The chiral material exhibits a large second harmonic generation (SHG) response of 13.5 × KDP (600 × α-SiO_2), and the shortest absorption edge (250 nm) of reported materials with a strong SHG response (>10 × KDP). PMTP has a three-dimensional crystal structure of corner-shared MgO_4, PO_4, and TeO_6 polyhedra, which form a $[TeMg_3P_2O_{14}]_\infty$ framework. Electronic structure calculations revealed that the stereoactive lone pair on the Pb^{2+} cation is critical to producing the substantial NLO response and that the NLO activity is further enhanced by the presence of triply bidentate Te^{6+} cations found in Te−O−O−Pb rings.

Nonlinear optical (NLO) materials are critical in generating coherent light through frequency conversion, e.g., second-harmonic generation (SHG). From the ultraviolet (UV) to the infrared (IR), NLO materials have expanded the range of the electromagnetic spectrum accessible by solid-state lasers.[1−6] With respect to UV NLO materials (λ < 400 nm), borates such as β-BaB_2O_4 (β-BBO),[6a] LiB_3O_5 (LBO),[6b] $CsLiB_6O_{10}$ (CLBO),[6c] and $KBe_2BO_3F_2$ (KBBF)[4] are often used. Each of these materials has drawbacks, thus requiring the discovery and characterization of new UV NLO materials.[7−17] For example, the large birefringence of β-BBO (Δn = 0.113 at 1064 nm) results in a large walk-off angle, whereas the small birefringence of LBO (Δn = 0.0399 at 1064 nm) limits the phase-matching wavelength. With CLBO, the softness and hygroscopic nature of the material makes the crystal difficult to cut and polish,[8] whereas for KBBF the need for toxic BeO in the synthesis and the layered crystal habit have limited its use.[4]

In addition to a short absorption edge, a number of other criteria must be satisfied for a viable UV NLO material.[1] These include (i) moderate birefringence (0.05−0.10), (ii) stability in air and non-hygroscopic behavior, (iii) large powder SHG (PSHG) responses, and (iv) facile growth of large crystals. It has been recently suggested that phosphates may be viable UV NLO materials, motivated by recent syntheses of crystals exhibiting short absorption edges: $Ba_3P_3O_{10}X$ (180 nm for X = Cl and <200 nm for X = Br),[9] $RbBa_2(PO_3)_5$ (163 nm),[10a] $Rb_2Ba_3(P_2O_7)_2$ (<200 nm),[10a] $Ba_5P_6O_{20}$ (167 nm),[10b] and $CsLa(PO_3)_4$ (167 nm).[11] However, these materials exhibit very weak PSHG responses because of the lack of NLO-active structural units, thus limiting their UV NLO applications. As has been done in other materials families, the introduction of NLO-active structural units into non-centrosymmetric phosphates could enhance their utility as UV NLO materials. NLO-active structural units include d^0 cations in distorted polyhedra,[12] polar chalcogenide units,[12] and stereochemically active lone pair (SCALP) cations.[13] However, using d^0 cations or chalcogenides causes a red shift of the absorption edge, rendering the material unsuitable for UV NLO applications. A SCALP cation also causes a red shift of the absorption edge, but often not so severely that UV NLO applications become inaccessible.

Because the presence of multiple NLO-active structural units should synergistically impact and enhance the SHG response,[13,14a,15] we focused on combining a phosphate group with a SCALP cation, Pb^{2+}, as well as Mg^{2+} and Te^{6+} cations. As reported earlier, acentric phosphates have very short absorption edges, and the inclusion of Pb^{2+} and Te^{6+} may enhance any SHG response. In addition, the Mg^{2+} cations should provide structural and thermal stability to the material. With all of this in mind, we successfully synthesized and characterized $Pb_3Mg_3TeP_2O_{14}$ (PMTP). PMTP exhibits a UV absorption edge of 250 nm and a very strong SHG response of ∼13.5 × KDP with 1064 nm incident radiation. PMTP has the shortest absorption edge among the known materials with strong SHG responses (>10 × KDP), i.e., β-$BaTeMo_2O_9$,[12c] $Na_2Te_3Mo_3O_{16}$,[16a] $Li_2Ti(IO_3)_6$,[13c] $BiO(IO_3)$,[13a] $Na_2Ti(IO_3)_6$,[15] $ZnTeMoO_6$,[16b] $MgTeMoO_6$,[16c] $Na_2TeW_2O_9$,[16d] $BaNbO(IO_3)_5$,[12b] $CdTeMoO_6$,[16e] $Pb_2B_5O_9I$,[13b] $Cd_4BiO(BO_3)_3$,[14a] and $CsPbCO_3F$.[17] In addition, PMTP is also stable to 1000 °C in air. Electronic structure calculations revealed that the Pb^{2+} SCALP cations play the largest role in the NLO response with the triply bidentate Te^{6+} cations also contributing, whereas rotations of the MgO_4 and PO_4 polyhedral units serve to lift the inversion symmetry. Here we report the synthesis, crystal growth, NLO properties, and electronic structure of PMTP. The experimental results and theoretical calculations indicate that PMTP is an excellent candidate for UV NLO applications.

Pure polycrystalline PMTP was synthesized by solid-state techniques at 850 °C (see the Supporting Information). The

Received: November 8, 2015
Published: December 19, 2015

DOI: 10.1021/jacs.5b11712
J. Am. Chem. Soc. 2016, 138, 88−91

phase purity was confirmed by powder X-ray diffraction (PXRD) (Figure S1). TG/DTA curves revealed an endothermic peak around 1093 °C accompanied by weight loss on the heating cycle, and there were two exothermic peaks at 751 and 820 °C on the cooling cycle (Figure S3). PXRD indicated that $Pb_3(PO_4)_2$, $Mg_3(PO_4)_2$, and other unknown phases (Figure S4) were recovered, suggesting that PMTP melts incongruently.

PMTP single crystals were grown from a high-temperature solution with TeO_2 as the flux, and the structure was determined by single-crystal XRD (Table S1). PMTP crystallizes in the chiral, non-centrosymmetric trigonal space group *P*321 (crystal class 32). The material is related to the natural occurring mineral dugganite.[18] PMTP exhibits a three-dimensional (3D) structure consisting of MgO_4 and PO_4 tetrahedra and $Te^{VI}O_6$ octahedra. Each MgO_4 tetrahedron shares two oxygen atoms with two different PO_4 tetrahedra, and each PO_4 tetrahedron shares three oxygen atoms with three distinct MgO_4 tetrahedra. Thus, a $[Mg_3P_2O_{14}]_\infty$ layer in the *ab* plane is observed. These layers are connected along the *c* axis by TeO_6 octahedra to create the 3D $[TeMg_3P_2O_{14}]_\infty$ framework (Figure 1). The Pb^{2+} cations are

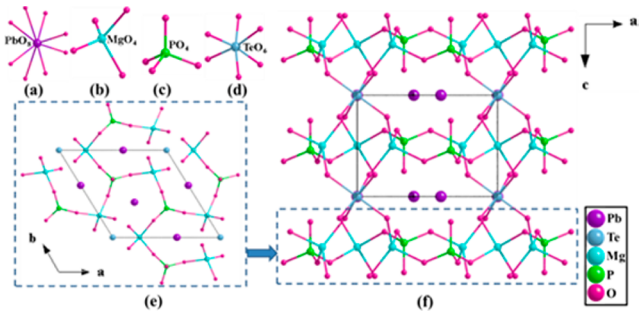

Figure 1. Crystal structure of PMTP: (a) PbO_8 polyhedron; (b) MgO_4 tetrahedron; (c) PO_4 tetrahedron; (d) TeO_6 octahedron; (e) $[Mg_3P_2O_{14}]_\infty$ layer; (f) 3D $[TeMg_3P_2O_{14}]_\infty$ framework.

located in the framework cavities. In connectivity terms, PMTP may be described as $\{[TeO_{6/2}]\ 3[MgO_{4/2}]^{2-}\ 2[PO_{3/2}O_{1/1}]\}^{6-}$ with the charge balanced by the three Pb^{2+} cations.

Each Mg (P) atom is bonded to four oxygen atoms with distances of 1.939(4)−1.957(4) Å (1.528(8)−1.539(4) Å). The Te^{6+} cations are bonded to six O atoms in an octahedral environment with a uniform bond length of 1.916(4). The Pb^{2+} cations are coordinated by eight O atoms with two short Pb−O bond lengths of 2.354(4) Å and six longer Pb−O bond lengths of 2.804(4)−2.933(13) Å. The variable Pb−O bond lengths suggest that the lone pair on each Pb^{2+} cation is stereochemically active (Figure S5). Bond valence calculations[19] gave values of 1.82, 2.01, 6.02, and 4.98 for Pb^{2+}, Mg^{2+}, Te^{6+}, and P^{5+}, respectively. The O valences range from 1.66 to 2.04.

PSHG measurements on PMTP with 1064 nm radiation revealed a very strong SHG efficiency of ~13.5 × KDP (600 × α-SiO_2). The material is also SHG-active with 532 nm radiation (Figure S6). Measurements of SHG intensity versus particle size indicated that PMTP is type-I phase-matchable (see Figure 2a).[20] The SHG response of PMTP is stronger than those of SHG-enhanced borates, carbonates, and nitrates and is compatible with those of d^0-cation-containing molybdates, tungstates, and SCALP-containing iodates and tellurites (see Table 1). The diffuse-reflectance spectrum indicates that PMTP has a relatively short absorption edge of ~250 nm (Figure 2b). The absorption edge is shorter than those of recently reported materials with very strong SHG responses (>10 × KDP), including molybdates,

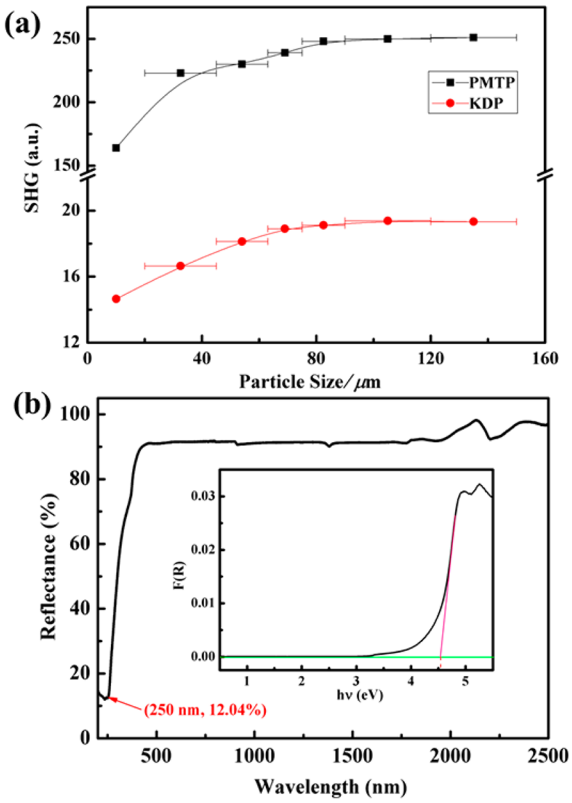

Figure 2. Linear and nonlinear optical properties of PMTP. (a) Phase-matching curve for PMTP. The solid curve is a guide for the eyes, not a fit to the data. (b) Diffuse-reflectance spectra of PMTP.

Table 1. PSHG Responses at 1064 nm and UV Cutoff Edges of Materials with Very High SHG Efficiencies

material	SHG (×KDP)	d_{ij} (pm/V)	abs. edge (nm)
β-$BaTeMo_2O_9$[12c,21]	13.6[12c]	d_{31} = 9.88,[a,21] d_{32} = −2.26,[a,21] d_{33} = 4.57,[a,21] d_{14} = −3.13[a,21]	500[12c]
$K(VO)_2O_2(IO_3)_3$[12a]	29.9[12a]	d_{14} = 23.07[b,12a]	446[12a]
$Na_2Te_3Mo_3O_{16}$[16a]	11.0[16a]	d_{eff} = 18.2[c,16a]	420[16a]
$Li_2Ti(IO_3)_6$[13c]	11.0[13c]	d_{eff} = 26[c,13c]	413[13c]
$Pb_2B_5O_9I$[13b]	13.5[13b]	d_{15} = 16.6,[b,13b] d_{24} = 9.4,[b,13b] d_{33} = 1.8[b,13b]	400[13b]
$Cd_4BiO(BO_3)_3$[14a]	6.0[14a]	d_{11} = 3.21,[b,14a] d_{33} = 2.81[b,14a]	392[14a]
$BiO(IO_3)$[13a]	12.5[13a]	d_{eff} = 26[c,13a]	376[13a]
$Na_2Ti(IO_3)_6$[15]	9.0[15]	d_{eff} = 23[c,15]	375[15]
$LiNbO_3$[22]	13.6[22]	d_{31} = 5.95,[a,22] d_{22} = 3.07,[a,22] d_{33} = 34.4[a,22]	370[18]
$ZnTeMoO_6$[16b]	10.5[16b]	–[d]	345[16b]
$MgTeMoO_6$[16c]	12.5[16c]	–[d]	360[16c]
$Na_2TeW_2O_9$[16d]	11.0[16d]	d_{eff} = 26[c,16d]	360[16d]
$KTiOPO_4$ (KTP)[23]	8.3[23]	d_{31} = 6.5,[a,23] d_{32} = 5.0,[a,23] d_{33} = 13.7,[a,23] d_{24} = 7.6,[a,23] d_{15} = 6.1[a,23]	350[23]
$BaNbO(IO_3)_5$[12b]	14.0[12b]	d_{11} = 8.30,[b,12b] d_{12} = 8.89,[b,12b] d_{13} = 9.02,[b,12b] d_{15} = 8.64,[b,12b] d_{24} = 9.40,[b,12b] d_{33} = 9.48[b,12b]	350[12b]
$CdTeMoO_6$[16e]	16.6[16e]	d_{14} = 11.7[b,16e]	345[16e]
$CsPbCO_3F$[17]	13.4[17a] 6.8[17b]	d_{22} = 5.25[b,17a]	300[17a]
$Pb_3Mg_3TeP_2O_{14}$	13.5	d_{11} = 5.98, d_{12} = d_{26} = −5.98	250

[a]Measured SHG coefficients. [b]Calculated SHG coefficients. [c]Estimated from PSHG data. [d]Not reported.

DOI: 10.1021/jacs.5b11712
J. Am. Chem. Soc. 2016, 138, 88−91

tungstates, iodates, tellurites, and even SHG-enhanced borates, carbonates, and nitrates (Table 1). These results clearly demonstrate that PMTP is an excellent UV NLO material.

To better understand the origin of the optical properties in PMTP, we utilized a group-theoretical analysis along with first-principles electronic structure calculations. We first disentangled the various atomic displacements that break the inversion center by generating a hypothetical high-symmetry, centrosymmetric structure for PMTP in space group $P\bar{3}m1$. Then a symmetry-adapted mode decomposition was performed following the approach introduced in ref 7b. Two displacive modes were found to relate the hypothetical centrosymmetric structure with the observed $P321$ chiral phase. The first mode, characterized by the irreducible representation (irrep) Γ_1^-, is responsible for breaking the inversion symmetry. This mode consists of large displacements of the Pb (1.40 Å) and Mg (3.64 Å) atoms as well as O displacements that serve to form the MgO_4 tetrahedra, corner-connect the tetrahedra with the TeO_6 octahedra, and rotate the PO_4 units. The second mode, given by the irrep Γ_1^+, has the full symmetry of the centric phase and causes the O atoms to shift closer to the Mg^{2+}, P^{5+}, and Te^{6+} cations, decreasing the volumes of the MgO_4, PO_4, and TeO_6 polyhedra.

Next, the roles of these inversion-symmetry-lifting displacements on the electronic structure were investigated by calculation of the atomically resolved density of states. In the high-symmetry $P\bar{3}m1$ structure, the system is metallic with highly dispersive Pb 6p states ranging from −4 to 4 eV and Pb 6s states that are lower in energy at −8 eV (Figure 3a). Upon freezing in the Γ_1^- mode and lifting of inversion symmetry (Figure 3b), the material reveals insulating character. Freezing this mode also shifts the Pb 6p states to the bottom of the conduction band, allowing the Pb 6s states to form the top of the valence band, where they overlap with O 2p states. Following this analysis, it is clear that the Γ_1^- mode is fundamental for enabling the NLO properties of PMTP. The displacements of the Pb^{2+} atoms, arising as a consequence of their stereoactive lone pairs, generate the sharp band edges essential to the SHG.[24] Finally, freezing in the Γ_1^+ mode results in the density of states of the equilibrium $P321$ structure (Figure 3c); this mode serves to push the nonbonding, formally in-gap O 2p states into the valence band, producing the wide band gap required for optical transparency up to the UV region. Our calculations predict a band gap of 3.44 eV, which is smaller than the experimentally observed value of 4.96 eV[9,10,25] or 4.57 eV determined by converting the UV−vis−NIR diffuse-reflectance spectrum into absorbance with the Kubelka−Munk function[26] and extrapolating the linear part of the rising curve to zero (Figure 2b).[17a,27] Both values are consistent with the known underestimation by standard exchange−correlation functionals in density functional theory.[28]

We next computed the SHG coefficients (d_{ij}) for PMTP. Point group 32 allows for five nonzero coefficients in the SHG tensor, of which only two are independent: $d_{11} = -d_{12} = -d_{26}$ and $d_{14} = -d_{25}$. However, Kleinmann symmetry[29] reduces the allowed coefficients from five to three by enforcing the condition that $d_{14} = -d_{25} = 0$. We found very large coefficients of $d_{11} = -d_{12} = -d_{26} = 5.98$ pm/V. We then fixed the Pb^{2+} cations at the high-symmetry positions found in the centrosymmetric space group $P\bar{3}m1$ and recomputed the SHG tensor. This resulted in $d_{11} = -d_{12} = -d_{26} = 2.01$ pm/V, a drastic decrease of 66% in the NLO response, further indicating the important contribution of the Pb SCALP atoms to the NLO properties of this material.

Our analysis is in agreement with recent work showing that the presence of Pb^{2+} cations can drastically improve the NLO response in chiral materials because the electronic, as opposed to the structural, contribution to the SHG dominates when the crystal structure is non-centrosymmetric and nonpolar.[30] Furthermore, the authors showed that the presence of closed Pb−O−O−B rings also enhances this response.[31] In PMTP, the displacements of the Pb^{2+} cations, attributable to second-order Jahn−Teller effects, are always toward the Te^{6+} atoms, as indicated by the fact that the O 2p states overlapping with the Pb 6s states at −6.5 eV are almost exclusively from those oxygen atoms making up the TeO_6 octahedra (Figure 3c). The resulting coordination network shows the important aforementioned ring structure, with each Te^{6+} cation chelated with three Pb^{2+} atoms, each via two bridging oxygens. All of the Te^{6+} atoms therefore have three bidentate ligands (Figure 4), a type of atomic configuration that has also been shown to improve the NLO response.[32] The excellent SHG response of this material is therefore attributable to both of these chemical features being active; PMTP is both chiral and Pb-containing, while also exhibiting triple-bidendate complexes.

To summarize, we have designed and synthesized $Pb_3Mg_3TeP_2O_{14}$, a new chiral material that exhibits a strong second harmonic response, a short absorption edge in the UV region, type-I phase-matchability, and excellent stability in air. We have shown that the simultaneous presence of a chiral crystal

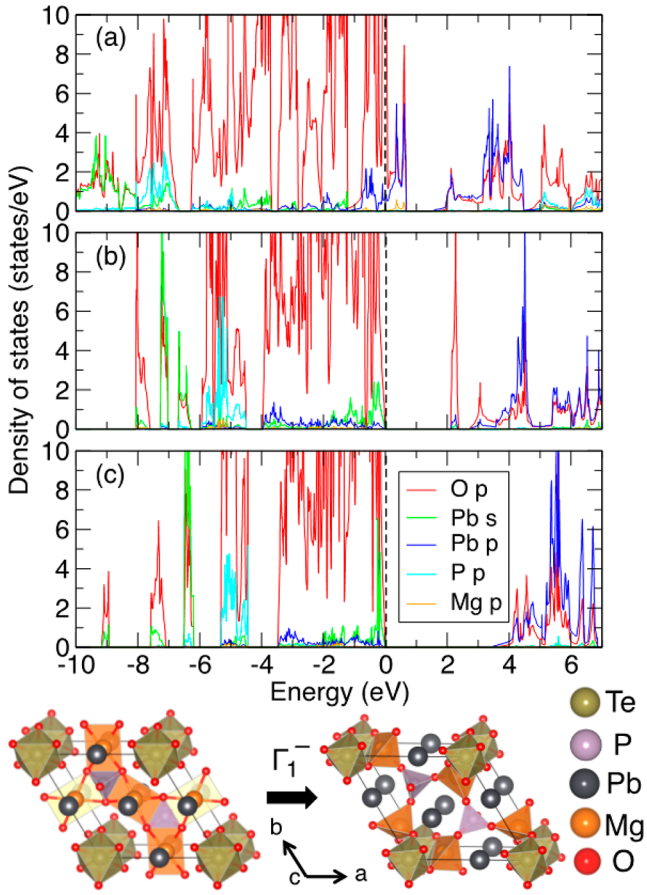

Figure 3. Atomically resolved density of states of PMTP (a) in the hypothetical high-symmetry centrosymmetric $P\bar{3}m1$ structure, (b) with the Γ_1^- mode frozen in, and (c) in the observed $P321$ structure. The atomic displacements making up the Γ_1^- mode are shown below (c). The O displacements described by the Γ_1^+ mode result in the differences between (b) and (c). The Fermi level (dashed vertical lines) is set at 0 eV.

DOI: 10.1021/jacs.5b11712
J. Am. Chem. Soc. 2016, 138, 88−91

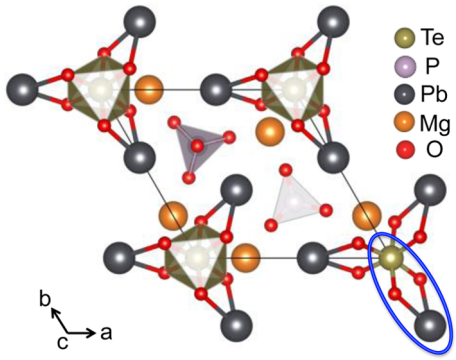

Figure 4. Ordering of the triply bidentate TeO_6 octahedra forming Te−O−O−Pb rings in the PMTP crystal structure (one such ring is circled in blue). Additional Pb−O bonds have been removed for clarity. The Te−O bonds are shown.

structure, stereoactive Pb^{2+} cations, and triply bidendate complexes, all key features in materials with large SHG responses, give rise to the excellent NLO properties of PMTP. We hope that this approach of targeted design can be harnessed to discover other new optically active materials, particularly in more difficult to reach regions of the electromagnetic spectrum.

■ ASSOCIATED CONTENT

Supporting Information

The Supporting Information is available free of charge on the ACS Publications website at DOI: 10.1021/jacs.5b11712.

Experimental details and additional data (PDF)
Crystallographic data (CIF)

■ AUTHOR INFORMATION

Corresponding Authors

*jrondinelli@northwestern.edu
*psh@uh.edu

Notes

The authors declare no competing financial interest.

■ ACKNOWLEDGMENTS

H.Y., W.Z., and P.S.H. thank the Welch Foundation (Grant E-1457) and NSF (DMR-1503573) for support. J.Y. and J.M.R. were supported by NSF (DMR-1454688). DFT calculations were performed on the CARBON cluster at the Center for Nanoscale Materials at Argonne National Laboratory, supported by DOE-BES (DE-AC02-06CH11357).

■ REFERENCES

(1) Becker, P. *Adv. Mater.* **1998**, *10*, 979.
(2) Keszler, D. A. *Curr. Opin. Solid State Mater. Sci.* **1996**, *1*, 204.
(3) Mori, Y.; Yap, Y. K.; Kamimura, T.; Yoshimura, M.; Sasaki, T. *Opt. Mater.* **2002**, *19*, 1.
(4) Chen, C.; Wang, G.; Wang, X.; Xu, Z. *Appl. Phys. B: Lasers Opt.* **2009**, *97*, 9.
(5) Chen, C.; Bai, L.; Wang, Z.; Li, R. *J. Cryst. Growth* **2006**, *292*, 169.
(6) (a) Chen, C. T.; Wu, B. C.; Jiang, A. D.; You, G. M. *Sci. Sin. B* **1985**, *15*, 235. (b) Chen, C. T.; Wu, Y. C.; Jiang, A. D.; Wu, B. C.; You, G. M.; Li, R. K.; Lin, S. J. *J. Opt. Soc. Am. B* **1989**, *6*, 616. (c) Mori, Y.; Kuroda, I.; Nakajima, S.; Sasaki, T.; Nakai, S. *Appl. Phys. Lett.* **1995**, *67*, 1818.
(7) (a) Yu, H.; Wu, H.; Pan, S.; Yang, Z.; Hou, X.; Su, X.; Jing, Q.; Poeppelmeier, K. R.; Rondinelli, J. M. *J. Am. Chem. Soc.* **2014**, *136*, 1264. (b) Wu, H.; Yu, H.; Yang, Z.; Hou, X.; Su, X.; Pan, S.; Poeppelmeier, K. R.; Rondinelli, J. M. *J. Am. Chem. Soc.* **2013**, *135*, 4215. (c) Wu, H.; Pan, S.; Poeppelmeier, K. R.; Li, H.; Jia, D.; Chen, Z.; Fan, X.; Yang, Y.; Rondinelli, J. M.; Luo, H. *J. Am. Chem. Soc.* **2011**, *133*, 7786. (d) Wang, S.; Ye, N. *J. Am. Chem. Soc.* **2011**, *133*, 11458. (e) Yu, H.; Wu, H.; Pan, S.; Yang, Z.; Su, X.; Zhang, F. *J. Mater. Chem.* **2012**, *22*, 9665.
(8) Karas, G. V. *New Developments in Crystal Growth Research*; Nova Science Publishers: New York, 2005.
(9) Yu, P.; Wu, L.-M.; Zhou, L.-J.; Chen, L. *J. Am. Chem. Soc.* **2014**, *136*, 480.
(10) (a) Zhao, S.; Gong, P.; Luo, S.; Bai, L.; Lin, Z.; Ji, C.; Chen, T.; Hong, M.; Luo, J. *J. Am. Chem. Soc.* **2014**, *136*, 8560. (b) Zhao, S.; Gong, P.; Luo, S.; Bai, L.; Lin, Z.; Tang, Y.; Zhou, Y.; Hong, M.; Luo, J. *Angew. Chem.* **2015**, *127*, 4291.
(11) Sun, T.; Shan, P.; Chen, H.; Liu, X.; Liu, H.; Chen, S.; Cao, Y. a.; Kong, Y.; Xu, J. *CrystEngComm* **2014**, *16*, 10497.
(12) (a) Sun, C.-F.; Hu, C.-L.; Xu, X.; Yang, B.-P.; Mao, J.-G. *J. Am. Chem. Soc.* **2011**, *133*, 5561. (b) Sun, C.-F.; Hu, C.-L.; Xu, X.; Ling, J.-B.; Hu, T.; Kong, F.; Long, X.-F.; Mao, J.-G. *J. Am. Chem. Soc.* **2009**, *131*, 9486. (c) Ra, H.-S.; Ok, K. M.; Halasyamani, P. S. *J. Am. Chem. Soc.* **2003**, *125*, 7764. (d) Yu, P.; Zhou, L.-J.; Chen, L. *J. Am. Chem. Soc.* **2012**, *134*, 2227. (e) Chen, M.-C.; Wu, L.-M.; Lin, H.; Zhou, L.-J.; Chen, L. *J. Am. Chem. Soc.* **2012**, *134*, 6058.
(13) (a) Nguyen, S. D.; Yeon, J.; Kim, S.-H.; Halasyamani, P. S. *J. Am. Chem. Soc.* **2011**, *133*, 12422. (b) Huang, Y.-Z.; Wu, L.-M.; Wu, X.-T.; Li, L.-H.; Chen, L.; Zhang, Y.-F. *J. Am. Chem. Soc.* **2010**, *132*, 12788. (c) Chang, H. Y.; Kim, S. H.; Halasyamani, P. S.; Ok, K. M. *J. Am. Chem. Soc.* **2009**, *131*, 2426.
(14) (a) Zhang, W. L.; Cheng, W. D.; Zhang, H.; Geng, L.; Lin, C. S.; He, Z. Z. *J. Am. Chem. Soc.* **2010**, *132*, 1508. (b) Inaguma, Y.; Yoshida, M.; Katsumata, T. *J. Am. Chem. Soc.* **2008**, *130*, 6704.
(15) Chang, H. Y.; Kim, S. H.; Ok, K. M.; Halasyamani, P. S. *J. Am. Chem. Soc.* **2009**, *131*, 6865.
(16) (a) Chi, E. O.; Ok, K. M.; Porter, Y.; Halasyamani, P. S. *Chem. Mater.* **2006**, *18*, 2070. (b) Zhao, S.; Luo, J.; Zhou, P.; Zhang, S.-Q.; Sun, Z.; Hong, M. *RSC Adv.* **2013**, *3*, 14000. (c) Zhang, J.; Zhang, Z.; Sun, Y.; Zhang, C.; Zhang, S.; Liu, Y.; Tao, X. *J. Mater. Chem.* **2012**, *22*, 9921. (d) Goodey, J.; Broussard, J.; Halasyamani, P. S. *Chem. Mater.* **2002**, *14*, 3174. (e) Zhao, S.; Jiang, X.; He, R.; Zhang, S.-q.; Sun, Z.; Luo, J.; Lin, Z.; Hong, M. *J. Mater. Chem. C* **2013**, *1*, 2906.
(17) (a) Zou, G.; Huang, L.; Ye, N.; Lin, C.; Cheng, W.; Huang, H. *J. Am. Chem. Soc.* **2013**, *135*, 18560. (b) Tran, T. T.; Halasyamani, P. S.; Rondinelli, J. M. *Inorg. Chem.* **2014**, *53*, 6241.
(18) Lam, A. E.; Groat, L. A.; Ercit, T. S. *Can. Mineral.* **1998**, *36*, 823.
(19) Brese, N. E.; O'Keeffe, M. *Acta Crystallogr., Sect. B: Struct. Sci.* **1991**, *47*, 192.
(20) (a) Kurtz, S. K.; Perry, T. T. *J. Appl. Phys.* **1968**, *39*, 3798. (b) Ok, K. M.; Chi, E. O.; Halasyamani, P. S. *Chem. Soc. Rev.* **2006**, *35*, 710.
(21) Yu, Q.; Gao, Z.; Zhang, S.; Zhang, W.; Wang, S.; Tao, X. *J. Appl. Phys.* **2012**, *111*, 013506.
(22) Sorokina, N. I.; Voronkova, V. I. *Crystallogr. Rep.* **2007**, *52*, 80.
(23) Dmitriev, V. G.; Gurzadyan, G. G.; Nikogosyan, D. N. *Handbook of Nonlinear Optical Crystals*; Springer: New York, 1999.
(24) Rondinelli, J. M.; Kioupakis, E. *Annu. Rev. Mater. Res.* **2015**, *45*, 491.
(25) Yao, W.; Huang, H.; Yao, J.; Xu, T.; Jiang, X.; Lin, Z.; Chen, C. *Inorg. Chem.* **2013**, *52*, 6136.
(26) Tauc, J. *Mater. Res. Bull.* **1970**, *5*, 721.
(27) Zhao, S. G.; Gong, P. F.; Bai, L.; Xu, X.; Zhang, S. Q.; Sun, Z. H.; Lin, Z. S.; Hong, M. C.; Chen, C. T.; Luo, J. H. *Nat. Commun.* **2014**, *5*, 4019.
(28) Baerends, E. J.; Gritsenko, O. V.; van Meer, R. *Phys. Chem. Chem. Phys.* **2013**, *15*, 16408.
(29) Kleinman, D. A. *Phys. Rev.* **1962**, *126*, 1977.
(30) Cammarata, A.; Zhang, W.; Halasyamani, P. S.; Rondinelli, J. M. *Chem. Mater.* **2014**, *26*, 5773.
(31) Dong, X.; Jing, Q.; Shi, Y.; Yang, Z.; Pan, S.; Poeppelmeier, K. R.; Young, J.; Rondinelli, J. M. *J. Am. Chem. Soc.* **2015**, *137*, 9417.
(32) Tran, T. T.; He, J.; Rondinelli, J. M.; Halasyamani, P. S. *J. Am. Chem. Soc.* **2015**, *137*, 10504.

DOI: 10.1021/jacs.5b11712
J. Am. Chem. Soc. 2016, 138, 88−91